Silver colloidal nanoparticles by electrochemistry: temporal evaluation and surface plasmon resonance

Silver colloidal nanoparticles by electrochemistry: temporal evaluation and surface plasmon resonance

H A Padilla-Sierra[1], **G Peña-Rodríguez**[1], **and G Chaves-Bedoya**[1]
[1] Grupo de Investigación en Instrumentación y Física de la Materia Condensada, Universidad Francisco de Paula Santander, San José de Cúcuta, Colombia

E-mail: angelikpad@gmail.com

Abstract. The electrochemical technique for obtaining silver nanoparticles has advantages over other methods. For the synthesis, a colloidal silver generator (Colloidal Silver Generator® model 1001) was used, where two electrodes coupled to high purity silver rods (99.99%) were used, with a potential difference of 24 V. Nanoparticle concentration was measured by total dissolved solids, using the SI-Analytic HandyLab 680 FK multiparameter in 200 mL of Milli-Q deionized water, reporting 18 ppm at 1 hour at room temperature. The determination of the resonance wavelength of the surface plasmons was carried out by finding the maximum absorbance by UV-Visible spectrophotometry with $\lambda = 423$ nm. The morphology and size of the nanoparticles was determined by Transmission Electron Microscopy, observing spherical morphology and sizes smaller than 50 nm. The chemical composition was determined by X-ray energy dispersed spectroscopy, finding a weight concentration of 93.22% of silver. The results show an optimal synthesis of colloidal silver, with characteristics that will allow the inhibition of microorganisms of interest.

1. Introduction

The silver nanoparticles (AgNPs) have been used in various fields, with medical and biotechnological applications, among others [1]. Its main interest, in addition to being considered an abundant and inexpensive natural resource, are its properties and characteristics, such as size, distribution, shape, composition and crystallinity, which is why it has been included in antibacterial and anticancer therapies [2].

They are generally synthesized by physical, chemical, and biological methods and due to their applications in different areas, several methods are proposed to obtain AgNPs of wide-range surface morphology [3], such as the laser ablation technique, thermal decomposition, electron irradiation and gamma, solgel, electrochemical and chemical reduction, among others [4,5]. Electrochemical synthesis is the most popular and economical [3], with advantages such as obtaining high purity colloidal solutions, with the possibility of controlling the size, allowing the choice of electrolytes with dispersing agents and surfactants [6]. The size of the nanoparticles is regulated by controlling parameters such as the concentration of electrolytes, the applied current density, and the separation between the electrodes [4]. In addition to obtaining a certain size and shape, it is an ecological method, since the process avoids the use of reducing agents that could become toxic [7].

Due to their antimicrobial properties, the most current use of AgNPs has been to include them in products for human and animal consumption, where they have raised concern for ecologists, since once released in water effluents, AgNPs can undergo oxidation processes contributing water toxicity. One of

the disadvantages is that silver can be deposited on the electrodes, passivating them, and effectively reducing the surface, reducing the generation of AgNPs colloids in the electrolyte [6-8]. For example, it has been reported that the decrease in the dissolved mass of Ag^+ ions in drinking water could be due to the reaction between them and Cl^-, forming silver chloride (AgCl) [7,8].

In general, the characterization of AgNPs suspensions is necessary, where robust instrumental techniques are used that allow the verification of the composition such as energy dispersed X-ray spectroscopy (EDS); nanoparticle concentration using total dissolved solids (TDS), surface plasmon resonance by absorption spectroscopy in the ultraviolet-visible (UV-Vis) range and morphology by transmission electron microscopy (TEM) and scanning electron microscopy (SEM), among others [9], which together with cytotoxic characterization allows its use in various industrial applications.

For this, the electrochemical synthesis of AgNPs and their morphological, structural and compositional characterization are proposed, using TEM, SEM, EDS and absorbance by spectrophotometry in the UV-Vis range, to evaluate the obtaining of nanoparticles free of other compounds and to determine the presence of spherical morphology and size less than 100 nm, characteristics that are related to disturbances at the level of the wall, cell membrane, permeability alterations, cellular respiration and leading to the death of microorganisms. These solutions, after obtaining and verification, are proposed to be used in gram-positive and gram-negative bacteria inhibition assays [10].

2. Materials and methods

The AgNPs were synthesized at room temperature using the method proposed by Khaydarov [7]. Two high purity (99.99%) silver cylindrical rods (goodfellow®), 10 cm in length and 3 mm in diameter separated by 2 cm were used as electrodes and coupled to a generator (Colloidal Silver Generator® model 1001), with a potential difference of 24 V. The system used for the synthesis of AgNPs is shown in Figure 1.

(a) (b)

Figure 1. Silver Generator® model 1001 colloidal system, used for the synthesis of AgNPs at room temperature. (a) Coloidal silver generator model 1001; (b) Silver nanoparticle solution.

A quantity of 200 mL Milli-Q deionized water was used as the electrolytic medium. The total time for the synthesis was 1 hour. TDS value was determined every 5 minutes using the multi-parameter HandyLab 680 FK from SI-Analytics ®, the growth rate of AgNPs over time in the electrolytic solution was measured using the Microcal Origin software version 6.0.

The resonance wavelength of the AgNPs surface plasmons was analyzed by maximum absorbance by spectrophotometry in the UV-Vis range, using a Thermo Scientific® GENESYS 10S series spectrophotometer. A series of dilutions were made by triplicate at 2 mg/L, 4 mg/L, 6 mg/L, 8 mg/L, 10 mg/L, 12 mg/L, 14 mg/L and 16 mg/L which allowed us to construct the AgNPs calibration curve, according to the Lambert Beer law [11].

The morphology of AgNPs was studied using TEM, (TEM-Tecnai G2 F20 equipment, FEI Quanta), with a field emission source of 0.1 nm resolution at 200 KV, and a maximum magnification 1.0 MX, coupled to the GATAN US 1000XP-P camera, and to the EDX Oxford Instruments XMAX Detector, with which the elemental chemical composition was determined by means of EDS. The sample was prepared by taking a drop of the solution and placed on a copper grid with carbon membrane (Lacey carbon/carbon 200). The size behavior of the AgNPs was analyzed using the images obtained from the TEM, and the free ImageJ software ImageJ. Analysis was performed according to the protocol reported by [12].

3. Results and discussion

The growth behavior of the AgNPs in the electrolytic medium as a function of time is shown in Figure 2. The best linear adjustment ($R^2 = 0.98$) to experimental data obtaining a slope with a value of 0.32 mg/min L, which represents the synthesis speed of the AgNPs in suspension.

On the other hand, it is appreciated that at 1 hour of the process 18 ppm (mg/L) of nanoparticles suspended in water are recorded. From this concentration, triplicate dilutions were made at 2 ppm, 4 ppm, 6 ppm, 8 ppm, 10 ppm, 12 ppm, 14 ppm and 16 ppm, in order to perform the calibration curve of the sample using the absorbance measured by spectrophotometry in the range UV-Vis, for which the sample was scanned with 14 ppm in the wavelength range of 350 nm to 525 nm (Figure 3). The resonance wavelength of AgNPs Plasmons depends on the shape and size between 350 nm and 450 nm [13]. The maximum absorbance was obtained for a wavelength of 423 nm, being consistent with that reported in the literature (Figure 3).

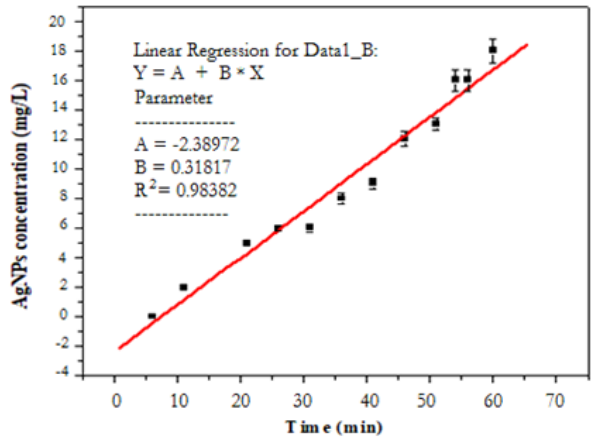

Figure 2. AgNPs concentration (mg/L) as a function of time (min). The line represents the best linear fit to the experimental data.

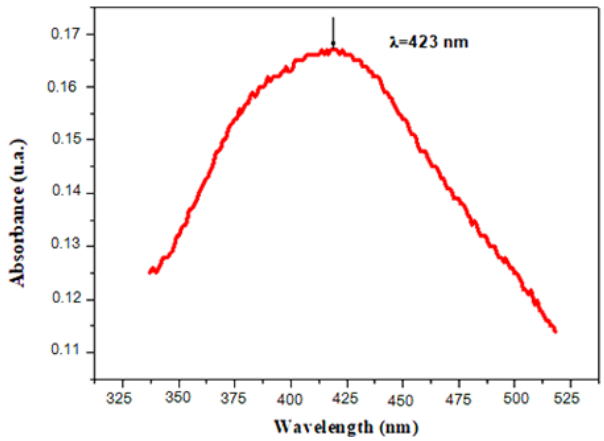

Figure 3. Absorption spectrum for the AgNPs sample diluted to 14 ppm, using a Thermo Scientific® GENESYS 10S series UV-Vis spectrophotometer.

The calibration curve of the absorbance for $\lambda = 423$ nm, of the different dilutions is shown in Figure 4, where the linearity is appreciated following the Lambert Beer´s law. The adjustment correlation coefficient is very close to one, giving validity to the experimental adjustment.

TEM images for AgNPs show a virtually spherical particle with an average size distribution of 5.63 nm $\pm$ 2.91 nm (minimum 1.56 nm and maximum 12.85 nm) information obtained using ImageJ software for one hundred particles taken from Figure 5(a) and Figure 5(b). Likewise, the largest and smallest amount of nanoparticles are in the ranges of 3 nm to 4 nm, and 7 nm to 8 nm respectively, as well as a bimodal behavior can be inferred by making a log-normal adjustment to the histogram, the first with a peak at 3.5 nm and the second at 9.5 nm (Figure 6).

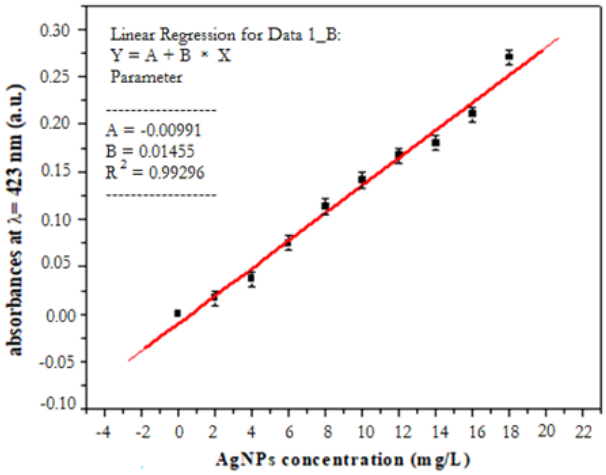

Figure 4. Calibration curve of the absorbance as a function of the concentration (mg/L) of AgNPs. Obtained by absorption spectroscopy in the UV-Vis range, for $\lambda = 423$ nm. The solid line represents the best fit to the experimental data with $R^2 = 0.99$.

The spherical morphology of the AgNPs observed in Figure 5, is justified in the synthesis process, where the formation of nanoparticles in the solution is initiated by the oxidation of the anode, forming Ag^+ ions, followed from the release of oxygen due to the electrolysis of water, creating a layer of Ag_2O on the surface of the anode. Then towards the cathode there will be migration of Ag^+ ions, generating atoms of it with zero valence. This is accompanied by the release of hydrogen and the formation of AgNP due to nucleation and growth by attractive Van der Waals forces between the atoms [6].

When comparing the results of the nanoparticles size distribution with the absorbance, spherical AgNPs with sizes less than 7 nm have a maximum absorbance peak around $\lambda = 410$ nm, and that as the average size of the nanoparticles increases, this peak of maximum absorbance moves to wavelengths in the range of 425 nm [14], this justifies finding a wavelength of maximum absorbance for sintered AgNPs in 423 nm.

In general, given the average size reported for AgNPs, a high proportion of Ag atoms on the surface of nanoparticles is evident, which can be used in a wide range of technological applications, including the treatment of pathogens that affect different crops and agro-industrial processes [15-17].

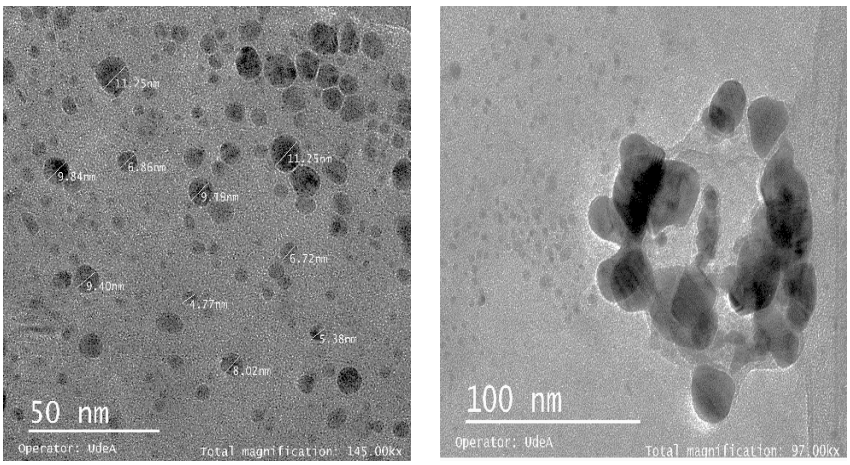

(a) (b)

Figure 5. TEM Images of the AgNPs. (a) 145 KX; (b) 97 KX.

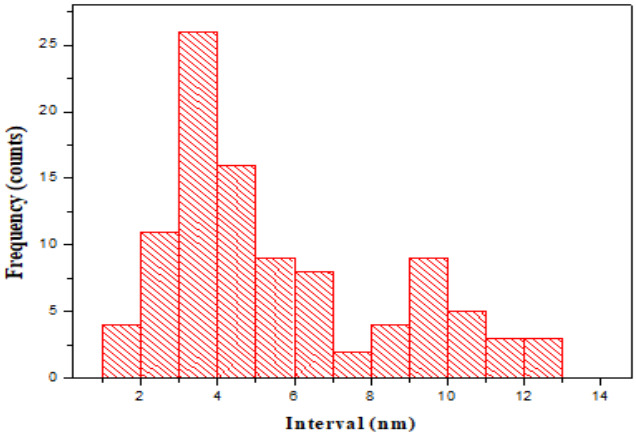

Figure 6. Frequency histogram for particle size.

The chemical microanalysis of AgNPs is presented in Figure 7. For its quantification, the concentration by weight of copper was eliminated, since this contribution corresponds to the grid of the same element in the sample holder. This analysis shows that the concentration of silver in percentage by weight of the sample is of the order of 93.22%.

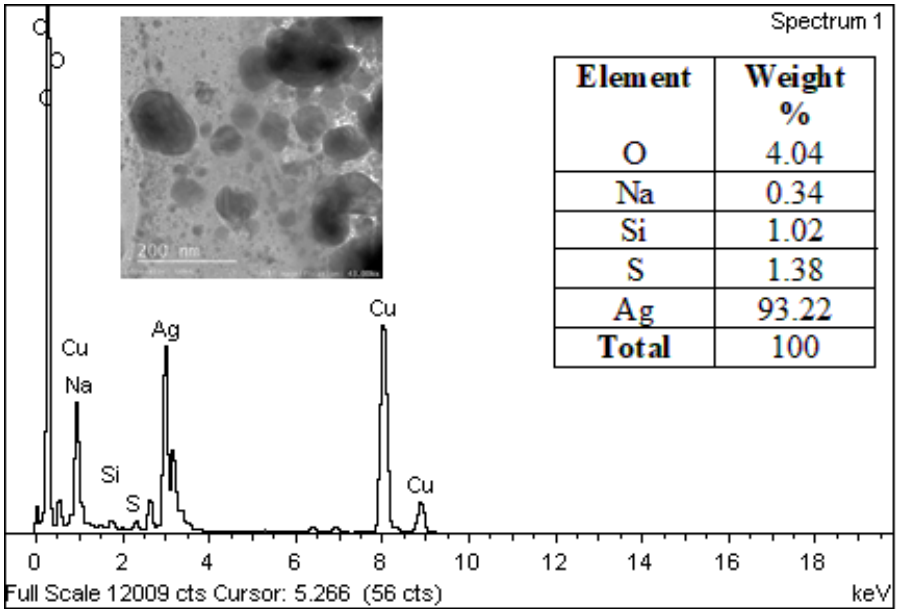

Element	Weight %
O	4.04
Na	0.34
Si	1.02
S	1.38
Ag	93.22
Total	100

Figure 7. X-ray energy scattering spectrum for AgNPs.

4. Conclusions

High purity silver nanoparticles were sintered at room temperature by electrochemistry using silver electrodes with the synthesis speed of 0.32 ppm/min, and with a maximum concentration of 18 ppm for a time of one hour. Almost spherical morphology was evidenced with an average particle size of 5.63 nm $\pm$ 2.91 nm and a bimodal particle size distribution with two maxima, one at 3.5 nm and the other at 9.5 nm.

The maximum absorbance (UV-Vis) of the AgNPs plasmons corresponds to a wavelength of 423 nm. The elemental composition of silver with a weight percentage of 93.22%, is optimal for use in technological, agro-industrial, and microbiological applications and especially for the possible inhibition of pathogens present in different crops and water effluents.

References

[1] Nasretdinova G, Fazleeva R, Mukhitova R, Nizameev I, Kadirov M, Ziganshina A, Yanilkin V 2015 Electrochemical synthesis of silver nanoparticles in solution *Electrochemistry Communications* **50** 69
[2] Lee S H, Jun B H 2019 Silver nanoparticles: synthesis and application for nanomedicine *International Journal of Molecular Sciences* **20(4)** 865
[3] Singaravelan R, Bangaru-Sudarsan A 2015 Electrochemical synthesis, characterisation and phytogenic properties of silver nanoparticles *Applied Nanoscience* **5(8)** 983
[4] Long D, Wu G, Chen S 2007 Preparation of oligochitosan stabilized silver nanoparticles by gamma irradiation *Radiation Physics and Chemistry* **76(7)** 1126
[5] Navaladian S, Viswanathan B, Viswanath R P 2007 Thermal decomposition as route for silver nanoparticles *Nanoscale Research Letters* **2** 44
[6] Khaydarov R A, Khaydarov R R, Gapurova O, Estrin Y, Scheper T 2009 Electrochemical method for the synthesis of silver nanoparticles *Journal of Nanoparticle Research* **11(5)** 1193
[7] Haider M, Mahdi M 2015 Synthesis of silver nanoparticles by electrochemical method *Engineering and Technology Journal* **33(7)** 1361
[8] Radwan I, Gitipour A, Potter P, Dionysiou D, Al-Abed S 2019 Dissolution of silver nanoparticles in colloidal consumer products: effects of particle size and capping agent *Journal of Nanoparticle Research* **21(7)** 155
[9] Cárdenas-Flechas L, Barba-Ortega J, Joya M 2020 Películas de óxido de cobre y hierro depositadas en nanotubos de titanio *Revista UIS Ingenierías* **19(1)** 171
[10] Shahverdi A R, Fakhimi A, Shahverdi H R, Minaian S 2007 Synthesis and effect of silver nanoparticles on the antibacterial activity of different antibiotics against Staphylococcus aureus and Escherichia coli *Nanomedicine: Nanotechnology, Biology and Medicine* **3(2)** 168
[11] Liu P, Chen G 2014 *Porous Materials Processing and Applications* (Waltham:Butterworth-Heinemann**)**
[12] Campa V M 2007 *Análisis de Imágenes de Microscopía con ImageJ* (Scotts Valley: Create-Space Publishing)
[13] Amendola V, Bakr O, Stellacci F 2010 Study of the surface plasmon resonance of silver nanoparticles by the discrete dipole approximation method: Effect of shape, size, structure, and assembly *Plasmonics* **5(1)** 85
[14] Martínez F, Zuñiga E, Sánchez A 2015 Método de síntesis de nanopartículas de plata adaptable a laboratorios de docencia relacionado con la nanotecnología *Mundo Nano* **6(10)** 101
[15] Vila A, Ayerbe R, Miró A, Rodríguez Á, Smani Y 2020 Antibacterial activity of colloidal silver against gram-negative and gram-positive bacteria *Antibiotics* **9(1)** 36
[16] Dakal T C, Kumar A, Majumdar R S, Yadav V 2016 Mechanistic basis of antimicrobial actions of silver nanoparticles *Frontiers in Microbiology* **7**
[17] Chiranjeevi N, Kumar P, Jayalakshmi R, Hari K, Prasad T 2018 Bio efficacy of biogenic silver nanoparticles against rice sheath blight causing pathogen *rhizoctonia solani* kuhn *International Journal of Current Microbiology and Applied Sciences* **7(7)** 4148